SAND2018-13356C

19PFL-0280

Combustion-Timing Control of Low-Temperature Gasoline Combustion (LTGC) Engines by Using Double Direct-Injections to Control Kinetic Rates

Author, co-author (Do NOT enter this information. It will be pulled from participant tab in MyTechZone)

Affiliation (Do NOT enter this information. It will be pulled from participant tab in MyTechZone)

Abstract

Low-temperature gasoline combustion (LTGC) engines can provide high efficiencies and extremely low NOx and particulate emissions, but controlling the combustion timing remains a challenge. This paper explores the potential of Partial Fuel Stratification (PFS) to provide fast control of CA50 in an LTGC engine. Two different compression ratios are used (CR=16:1 and 14:1) that provide high efficiencies and are compatible with mixed-mode SI-LTGC engines. The fuel used is a research grade E10 gasoline (RON 92, MON 85) representative of a regular-grade market gasoline found in the United States. The fuel was supplied with a gasoline-type direct injector (GDI) mounted centrally in the cylinder. To create the PFS, the GDI injector was pulsed twice each engine cycle. First, an injection early in the intake stroke delivered the majority of the fuel (70 – 80%), establishing the minimum equivalence ratio in the charge. Then, a second injection supplied the remainder of the fuel (20 – 30%) at a variable timing during the compression stroke, from 200° to 315°-330°CA (0°CA = TDC-intake, 360°CA = TDC-compression) to provide controlled stratification. For both CRs, second DI timing sweeps were performed for a range of intake pressures from highly boosted to naturally aspirated conditions, allowing the CA50 control authority at each condition to be determined. By varying the late-DI timing, CA50 could be adjusted as much a 12°CA, from near the misfire limit (overly retarded CA50) to well beyond the acceptable knock/ringing limit (overly advanced CA50). For different conditions, the amount of DI timing retard and CA50 advancement was limited by either engine knock, combustion instabilities, or high NOx emissions. For most conditions, approximately 6-8°CA of CA50 control was possible with good stability and acceptable NOx emissions.

Introduction

Advanced low-temperature gasoline (LTGC) engines that operate by compression ignition of a highly dilute charge can achieve high thermal efficiencies comparable to modern diesel engines, and much higher than those of gasoline spark ignition engines (SI), particularly at low loads [1, 2]. Characteristics of LTGC include lower heat transfer

losses, a higher ratio of specific heats (γ), higher allowable expansion ratios, and lower pumping losses, all of which contribute to a high thermal efficiency. Although low-temperature combustion has been attempted with other fuels [3-5], gasoline works particularly well under low-temperature conditions; its volatility and reactivity allow the fuel and air enough time to mix prior to combustion to keep the overall equivalence ratio and combustion temperature low, mostly avoiding conditions that form significant amounts of soot and oxides of nitrogen (NOx) [6]. However, an oxidation catalyst will still likely be necessary to reduce unburned hydrocarbons and carbon monoxide emissions to acceptable levels. Nonetheless, since the soot and NOx emissions are managed in-cylinder with LTGC, the exhaust aftertreatment requirements are greatly reduced compared to conventional diesel combustion.

The most fundamental form of LTGC is homogeneous charge compression ignition (HCCI) in which the piston motion compresses a fully premixed charge of fuel and air to the point of autoignition, with low- and intermediate-temperature chemical kinetics controlling the start of the main combustion. For engine timescales, high-temperature kinetic pathways are generally fast, so once hot-ignition occurs for HCCI-like combustion, the heat-release rate (HRR) is primarily controlled by the amount of thermal stratification, with chemical kinetics playing a secondary role [7]. Although HCCI is “homogeneous” in the sense that the fuel and air are well mixed, there will always be some amount of thermal stratification in an engine because of heat transfer and turbulent structures transporting colder fluid throughout the bulk gas [8]. This naturally occurring thermal stratification is actually advantageous since it produces a staged ignition, with autoignition occurring sequentially from the hottest regions to the coldest [9, 10]. This reduces the peak HRR and propensity for engine knock, which is one of the main challenges for HCCI-like combustion as the fueling rate increases. In fact, researchers have been working on LTGC/HCCI for nearly 40 years [11, 12] addressing such technical barriers to implementing LTGC in a production engine. There has been significant progress in understanding the fundamentals, but controlling the combustion timing, particularly through transients, remains a major challenge.

Controlling the phasing between the allowable limits of knock and misfire can be difficult because the chemical kinetics of autoignition are very sensitive to the in-cylinder conditions including compressed-gas temperature, compressed-gas pressure, oxygen concentration, fuel molecular composition, and for some fuels, equivalence ratio [6, 13]. The autoignition kinetics are particularly sensitive to temperature, so the most straightforward technique to control the combustion timing is by heating the intake air [7], or by utilizing valve-timing strategies to retain hot residuals [14, 15]. However, one drawback is that because of the thermal inertia of the engine, and because cam profile switching is not particularly fast, controlling the temperature quickly enough to respond on a cycle-by-cycle basis to changing speed and load is quite challenging. Using cooled exhaust gases (EGR) is another well-known strategy to control the combustion phasing, which lowers the autoignition reactivity by reducing the oxygen concentration and temperature [16]. However, it is also difficult to quickly change the amount of EGR, and at low loads significant intake heating or retained hot residuals are needed without EGR. It should be noted that retaining hot exhaust products actually dilutes the mixture

and decreases the oxygen concentration, but the high temperatures generally dominate over the decrease in oxygen concentration. However, this may not be true at low loads when the exhaust enthalpy of the retained hot residuals may not be sufficient to ignite the charge without supplying additional intake heat [17].

In combination with intake temperature and EGR, fuel injection strategies that produce charge stratification show promise for controlling the combustion-timing of LTGC engines. With direct injection (DI) of the fuel, the DI timing can promote more or less fuel stratification, which can affect the combustion phasing and HRR if the autoignition timing is sensitive to the local equivalence ratio [18, 19]. Perhaps most importantly, for DI fueling the quantity of fuel and the injection timing can be adjusted from one cycle to the next, providing a fast response to changes in engine speed and load, which often requires a rapid shift in the combustion timing to prevent the engine from knocking or misfiring.

Injecting a gasoline-like fuel near TDC can create a highly stratified mixture, and advancing the injection timing from this point can allow more time for mixing to occur. Kalghatghi et al. [20-23] used this approach in a single-cylinder research engine with a 14:1 compression ratio (CR) using gasoline (95 RON, 86 MON), and operating at 1200 RPM, with an intake pressure (P_{in}) = 1.5 bar, and an intake temperature (T_{in}) = 40°C [20]. For an engine load of 5.5 bar Indicated Mean Effective Pressure (IMEP), the equivalence ratio was ϕ = 0.26, which did not require any EGR to prevent the combustion-phasing from becoming too advanced. Starting with a single direct injection at 15°CA before Top Dead Center (bTDC) and advancing the start of injection (SOI) up to 30°CA bTDC, the 50% burn point (CA50) was advanced with the advance SOI up to about 10°CA. However, injecting earlier than 30°CA bTDC caused the combustion phasing to become more retarded, eventually leading to misfire as the mixture became more well-mixed. Thus, for SOIs earlier than 30°CA bTDC, CA50 moved opposite of the SOI. NOx and soot emissions were reported to be low for the entire SOI sweep at these conditions. Johannsson and coworkers [2, 22-27] have also extensively investigated partially premixed combustion (PPC) using gasoline-like fuels and obtained similar results. That is, for SOIs earlier than a certain late-compression-stroke timing, CA50 becomes more advanced as the SOI is retarded, whereas for SOIs later than this particular timing, CA50 moves with SOI, as occurs in diesel combustion.

Sellnau et al. [28, 29] have also shown how the injection timing can control the combustion phasing in a prototype multi-cylinder LTGC engine. This engine has a 16:1 CR, variable valve timing to retain hot residuals, a cooled EGR system, and a supercharger and turbocharger to provide intake-pressure boost. The gasoline used was a typical pump gasoline that can be found in the United States (RON 91.7, MON 83.4). Running the engine at 1500 RPM at a moderate load of 6 bar IMEP, a double DI strategy was used to control the combustion phasing for various conditions. Keeping the timing of the first fuel pulse fixed, and sweeping the second DI timing starting from a relatively early point, the CA50 advanced as the second DI timing was retarded, providing about 7-8°CA of CA50 control from the most-retarded to the most-advanced points. A second-DI timing in this window provided high thermal efficiencies with low

NOx and soot emissions. However, similar to the behavior observed by Johannsson [26] and Kalghatghi [20], when the second-DI timing was retarded further, the trend in CA50 reversed, with CA50 becoming more retarded with a later second DI timing. Operation in this later second-DI regime was accompanied by higher NOx and soot emissions compared to levels obtained with DI timings before the CA50 reversal.

Dec and coworkers [1, 13, 18, 19, 30-33] have performed numerous studies of the effects of varying the injection timing in LTGC engines mainly using a technique called partial fuel stratification (PFS). PFS allows good combustion efficiency to be maintained while applying controlled stratification to reduce the HRR in order to obtain higher loads without knock and/or to reduce the required CA50 retard for higher efficiencies. With PFS, most of the fuel (typically on the order of 70-95%) is premixed or supplied with an early DI to avoid producing overly lean regions that have poor combustion efficiency[1] [19][34]. Then, the remainder of the fuel is delivered by a late-DI, typically in the latter half of the compression stroke, to provide the stratification. The timing and/or fuel-fraction of this late-DI fueling is adjusted to vary the amount of stratification. In most of these works, the late-DI timing or fuel fraction was limited to avoid overly stratified conditions that can lead to unacceptable NOx and soot emissions. Early efforts focused on understanding the role of fuel-chemistry in controlling the autoignition timing using PFS [18]. It was found that for fuels that are ϕ-sensitive, meaning that the autoignition timing is sensitive to the local equivalence ratio, richer regions autoignite faster than the leaner regions. When PFS is applied with these fuels, it results in a sequential autoignition from the richest region to the leanest, which increases the burn duration and reduces the peak HRR, reducing the propensity for engine knock [19]. In initial experiments at naturally aspirated conditions, a two-stage ignition fuel (PRF80) with low-temperature heat release (LTHR) was found to be ϕ-sensitive, while single-stage fuels iso-octane and gasoline were not[2] [18]. However, subsequent studies showed that gasoline became ϕ-sensitive with intake boost, even though it showed virtually no LTHR, but only enhanced intermediate temperature heat release (ITHR) [32, 35]. ITHR results from the early reactions that ramp the combustion up into hot autoignition [36] and as the name indicates, it occurs at temperatures below the hot-ignition temperature and above those of the low-temperature heat release (LTHR) if the latter is present. A subsequent analysis of data from both naturally aspirated and boosted operation showed that the ϕ-sensitivity correlated most strongly with the intensity of the ITHR, for all cases, even for those where LTHR was present [35]. Although the exact mechanism

---

[1] If mixtures are too lean or too dilute with EGR, combustion temperatures become so low (below 1500 K) that reaction rates are too slow for the bulk-gas CO-to-CO2 reactions to go to completion before the piston expansion quenches the combustion [34].

[2] In References [18,32], the ϕ-sensitivity was measured in an engine using an alternate-firing technique called “Fire 19/1” to isolate the fuel-chemistry from the thermal and thermodynamic effects of having a higher equivalence ratio (i.e. hotter wall temperatures, hotter residuals, and lower γ’s with increased equivalence ratios). With this firing technique, 19 cycles are fired at a baseline ϕ_m, followed by 1 cycle fired at the ϕ_m of interest, resulting in nearly constant wall and residual gas temperatures. The majority of the charge is premixed operating at the baseline ϕ_m, and an early DI fueling is used to increase the base equivalence ratio to the ϕ_m being tested. Because of the increased PRRs and HRRs with higher equivalence ratios when the charge is well mixed, the maximum equivalence ratio that can be tested in this manner is around $\phi_m \approx 0.48$.

is not well understood, this ITHR correlation has been found for all fuels and conditions studied. [34] [18] [32]

As mentioned above, when PFS is applied at conditions where the fuel is ϕ-sensitive, the richest regions autoignite faster followed by the next richest and so on to the leanest regions. In the earlier studies from our laboratory cited above, the main goal was to investigate the extent to which this sequential autoignition could improve LTGC performance and extend its operating range by reducing the HRR to allow higher loads without knock and/or to allow CA50 to be more advanced for higher efficiency. Because changing the combustion phasing strongly affects the HRR by itself, many of the experiments in these previous works (e.g [30, 32, 33]) were performed at a constant CA50 to isolate the effects of PFS on the HRR profile from CA50 effects so they could be more clearly understood. Thus, T_{in} or the amount of EGR was adjusted to compensate for changes in the combustion timing that would otherwise have been induced by the varying amounts of stratification. If no adjustments were made, the richer regions would autoignite even earlier than they did when CA50 was held constant. The combustion of these richest regions would then compress the remaining charge causing the next richest regions to autoignite earlier, and so on, advancing the entire combustion process, i.e. advancing CA50. Moreover, increasing the fuel stratification by further retarding the late-DI timing or increasing the late-DI fuel fraction, would further increase the equivalence ratio of the richest regions, causing even greater CA50 advancement. Therefore, it should be possible to control the CA50 timing by varying the amount of stratification produced by PFS. Also, because fuel-injection timings and amounts can be varied from one cycle to the next, this CA50 control should be essentially instantaneous.

The objective of this current work is to investigate the potential of PFS for providing rapid control of CA50 in an LTGC engine. In this study, a GDI (gasoline direct injection) fuel injector is used with 120 bar fuel pressure to supply double direct injections (D-DI) into the cylinder to create the PFS. The fuel used is a research-quality regular-grade E10 gasoline (RON 92, MON 85) representative of a pump gasoline found in the United States. The ability of PFS to control the combustion timing was explored for two compression ratios: CR=16:1 and CR=14:1. These same CRs have been used in previous LTGC studies from our lab [16, 37], and were chosen since both CRs offer high efficiencies and are considered to be compatible with hybrid SI-LTGC combustion strategies proposed by various automotive companies and research groups[3]. A higher compression ratio increases the pressure at TDC, which acts to increase the autoignition reactivity and ϕ-sensitivity, so the intake temperature (or hot residuals) can be decreased to a greater extent than to just to compensate for the additional compression heating. These lower temperatures increase the charge density and γ, which leads to a higher IMEP and thermal efficiency (TE). The increased expansion

[3] With hybrid SI-LTGC combustion strategies, SI combustion is used at high loads, with mode switching to LTGC at low to medium loads where LTGC is more efficient [14,41]. Various automotive companies and research groups consider a CR in the range of 12.5 to 16:1 to be a practical limit due to engine-knock during high-load SI operation.

ratio with CR=16:1 also acts to increase TE, and in a recent study [38], CR = 16:1 was shown to increase TE by about 1%-unit over CR=14:1 for 1.6 bar ≤ P_{in} ≤ 2.5 bar. For both CR=16:1 and 14:1, second DI timing sweeps are performed starting at a high boost pressure (P_{in}=2.0-2.4 bar) where the fuel is known to be ϕ-sensitive, and then at decreasing intake pressures down to P_{in} = 1.0 bar where it is not known if the fuel will have sufficient ϕ-sensitivity. For each P_{in}, the start of the second DI-timing sweep is near BDC, which results in a relatively well-mixed charge, then, the second DI-timing is retarded until CA50 is limited by engine knock, combustion instability, or high NOx emissions. The total range of CA50 control at each condition is reported and discussed.

The following section describes the single-cylinder research-engine facility used for the experiments and provides details about the engine configuration, the fuel injector hardware, and the D-DI fueling strategy employed. Fuel specifications and the data acquisition techniques used are also presented. The experimental results are then presented in two parts: the D-DI PFS results obtained with the CR = 16:1 piston are presented first, followed by the CR=14:1 results. Finally, the last section provides a summary of the main findings and some concluding remarks are made.

[14, 39, 40]

Experimental Setup

Engine Facility

The LTGC/HCCI research engine used for this study was derived from a Cummins B-series six-cylinder diesel engine, which is a typical medium-duty diesel engine with a displacement of 0.98 liters per cylinder. As shown in the schematic of the engine facility in Fig. 1a, the engine has been converted for single-cylinder operation by deactivating cylinders 1-5. The configuration of the engine and facility is nearly identical to those used in our previous studies involving intake pressure boost [38, 41] with the exception of the cylinder head, and the geometry of the CR = 14:1 piston. Figures 1b and 1c show drawings of the CR = 14:1 and 16:1 pistons used in the active LTGC cylinder, respectively. The CR = 16:1 piston is the same one used in all previous studies, but the CR = 14:1 piston has a broad shallow bowl similar to the CR = 16:1 piston, rather than the narrower bowl used in most recent studies [32, 35, 38, 41, 42] However, the current CR = 14:1 piston was previously used in Refs. [17, 37] , which provide a more complete discussion of the differences between these two CR = 14:1 pistons. Both the current CR = 14:1 and 16:1 pistons provide open combustion chambers with a large squish clearance and small top-land ring crevices.

In this study, a cylinder head that was modified to incorporate a spark plug was used as first described in Ref. [37]; it is referred to here as Head #2. The spark plug is not relevant to the experiments presented here, so it was removed and an AVL GH15D pressure sensor was installed in its place using a threaded adapter. The spark plug port

has 10 mm diameter threads 42 mm off-center and inclined at an angle of 27.2° from vertical. This is approximately the same location where the water-cooled pressure sensor was mounted in previous studies (AVL QC33C or QC34C) [1, 17, 42, 43]. These earlier studies used Head #1, which has a low-swirl = 0.9 obtained using an anti-swirl plate. Head #2 also has a low-swirl ratio of 0.7, but the low-swirl is a result of the intake-port design itself instead of an anti-swirl plate. This pressure sensor installed in the spark plug port provides the primary pressure signal used for the data analysis. A second AVL GH15D pressure sensor is also used that accesses the combustion chamber through the firedeck via a short horizontal port with a conical opening into the combustion chamber. AVL PH08 flame arrestors were installed on both sensors to prevent thermal shock to the diaphragm to maintain high accuracy and repeatability. Furthermore, during all experimental sweeps, the pressure traces from the two sensors were monitored and compared to each other as a check to see if the sensor calibrations were drifting.

Prior to running the experiments, the engine was preheated to 100°C by means of electrical heaters on the “cooling” water and lubricating-oil circulation systems. All data for this paper were taken at an engine speed of 1200 rpm. A summary of the engine specifications are provided in Table 1. For all data presented, 0° crank angle (CA) is defined as TDC intake (so TDC compression is at 360°). This eliminates the need to use negative crank angles or combined bTDC, aTDC notation.

Table 1. Engine configuration used in the experiments

Bore	102 mm
Stroke	120 mm
Connecting Rod Length	192 mm
Displacement	0.98 L
Compression Ratios used:	14:1, 16:1
Volume at TDC (14:1, 16:1)	75.43 cm^3 , 65.4 cm^3
Number of Valves	4
Intake Valve Opening (IVO)	0° CA
Intake Valve Closing (IVC)	202° CA
Exhaust Valve Opening (EVO)	482° CA
Exhaust Valve Closing (EVC)	8° CA
Swirl Ratio	0.7
Type of Fueling used	Direct Injection
Engine Speed	1200 RPM
Coolant and oil temperature	~ 100 °C
GDI Injector	Bosch HDEV 5.1 90° spray angle 8-stepped holes
Fuel Pressure	120 bar

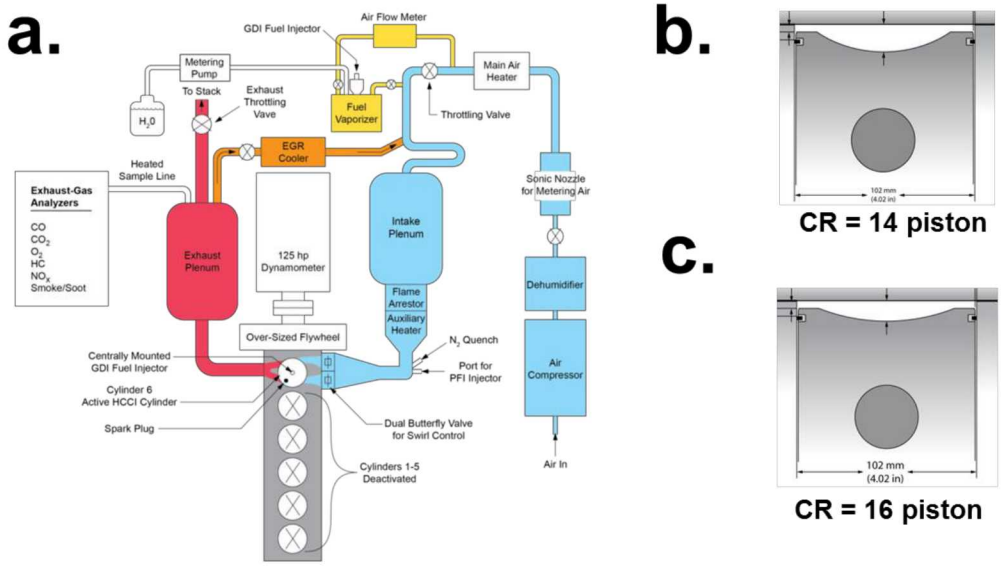

Figure 1. (a) Schematic of the LTGC (HCCI) Engine and subsystems (b) CR=14:1 piston (c) CR=16:1 piston

Airflow is supplied by an air compressor and precisely metered by a sonic nozzle as shown in Fig. 1a. After the sonic nozzle, a main heater provides some preheat if needed. All experiments in this article use DI fueling as discussed below. The facility is also equipped to provide premixed fueling using an electrically heated vaporizing chamber as shown in Fig. 1a, as has been used in many previous studies (e.g. [give 2 refs.]).

The insulated runner from the intake plenum to the engine is outfitted with a flame arrestor, an auxiliary heater, pressure sensors, and thermocouples. The auxiliary heater and thermocouples are mounted close to the engine to allow precise control of the T_{in}, which ranged from 60°C to 160°C for this study. For operation without EGR, the airflow was adjusted to achieve the desired intake pressure, which varied from 1.0 bar (simulating naturally aspirated conditions) to 2.4 bar for the current study.

As the intake-pressure is boosted, fuel reactivity increases [15, 19], and T_{in} must be reduced to compensate. For DI Fueling, there is not a need to consider fuel condensation, and T_{in} can be decreased to 30°C or 40°C (the lowest temperatures that can consistently be achieved in this laboratory, which are representative of the lower temperatures reached with an air intercooler). For operation with higher boost levels, T_{in} is held constant at (30-60°C), and cooled EGR is used to dilute the charge, reducing the autoignition propensity and preventing CA50 from becoming overly advanced.

After exiting the engine, the exhaust gases enter an insulated plenum before being vented out the exhaust stack, as shown in Fig. 1a. When EGR is used, some of the exhaust gases are recirculated back to the intake using a cooled EGR loop as also shown in Fig. 1a. With this configuration, the exhaust pressure must be greater than the intake pressure for EGR to flow into the intake system. The required backpressure is achieved by throttling the exhaust flow using the valve shown in the figure. The EGR is introduced into the intake-air upstream of a series of bends in the intake plumbing to ensure thorough premixing of the EGR and air. When the valve on the EGR loop is opened, the airflow is reduced from the amount required to achieve the desired intake pressure with air alone. The exhaust back-pressure throttle valve is then adjusted to produce enough EGR flow to reach the desired intake pressure. This typically resulted in the exhaust pressure being about 2-5 kPa greater than the intake pressure. At boosted conditions, for consistency the back pressure was maintained about 5 kPa above the intake pressure, even when EGR was not used. At naturally aspirated conditions, the exhaust back-pressure was left unthrottled. The flow rate of the cooling water for the EGR loop can be adjusted to control the temperature of the EGR gases to temperatures as low as 30°C. Furthermore, a water trap downstream of the EGR cooler removes the water that condenses if the EGR gases are cooled below their dew point.

Fuel Injection Schedule for PFS

In the current work, fuel was supplied by an eight-hole Bosch HDEV 5.1 gasoline-type direct injector (GDI) mounted centrally in the cylinder as shown in Fig. 1a. The fuel pressure was 120 bar, and other injector details may be found in Table 1.

For these PFS studies, the GDI injector was pulsed twice each engine cycle. The SOI of the first pulse will be referred to as SOI1, and the timing of the later second DI pulse will be referred to as SOI2 (see Fig.2). First, an injection early in the intake stroke, SOI1 = 60°CA, delivered the majority of the fuel (70 – 80%). Then, a second injection supplied the remainder of the fuel (20 – 30%) at a variable timing during the compression stroke, with SOI2 = 200° to 315°-330°CA, depending on the conditions. The onset of either engine knock, combustion instability, or high NOx, depending on the CR and P_{in}, limited the amount of SOI2 timing retard and correspondingly, the amount of CA50 advance. Figure 2 shows a plot of the cylinder volume and an example of the relative timing of the fuel pulses during the engine cycle.

A digital pulse/delay generator whose output was synchronized with the engine supplied the firing signal to the GDI injector driver. Using two separate output channels of the pulse/delay generator, the timings and durations of the two pulses were set independently and the two signals were combined with a logical “or” gate before being sent to the injector driver. The supplied amount of fuel was measured using a positive

displacement flow meter, and the fuel flow was adjusted until the desired charge-mass equivalence ratio was obtained.

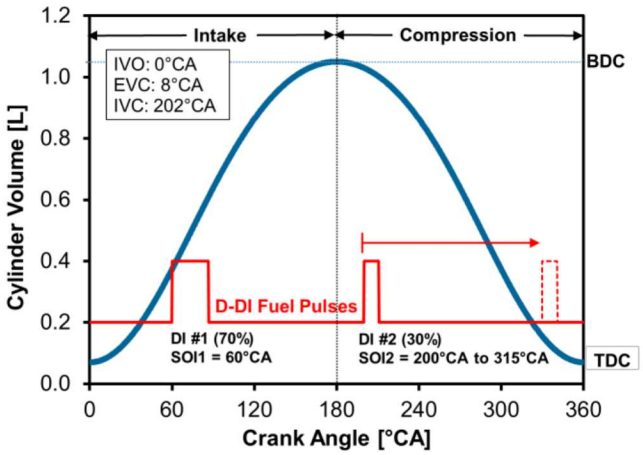

Figure 2. Cylinder volume and injection schedule for a D-DI 70/30 fuel split (70% at SOI1 = 60°CA, 30% at SOI2). The fuel pulses shown correspond to CR= 16:1, 1200 RPM, P_{in} = 2.0 bar, and ϕ_m = 0.40.

As discussed earlier, LTGC engines typically operate quite dilute to keep combustion temperatures low and to manage the high HRRs that can occur. Charge dilution is generally accomplished by using some combination of excess air, EGR, and/or retained residuals. For this reason, it is often convenient to compare mixtures with the same supplied energy content per charge mass by using a charge-mass based equivalence ratio (ϕ_m) to describe the mixture stoichiometry. This charge-mass equivalence ratio is defined as shown in Eq. 1.

$$\phi_m = \frac{\left({}^{F}/_{C}\right)}{\left({}^{F}/_{A}\right)_{stoich.}} \qquad (1)$$

Where F/C is the ratio of fuel mass to the total charge mass, and (F/A)stoich. is the fuel-to-air mass ratio for a stoichiometric mixture. It is important to note that when there are no exhaust or residual gases, ϕ_m is the same as the conventional air-based equivalence ratio (ϕ).

Fuel Specification

Since gasoline is a distillate fuel comprised of hundreds of different hydrocarbons, its composition can vary considerably from batch to batch. For research purposes, a gasoline with tighter specifications is needed to obtain repeatable results and to compare data with others who are performing similar research. The fuel used in this work is a research-grade E10 gasoline (RON 92, MON 85) named RD5-87 that has been used for recent research in industry, academia, and at national laboratories [37, 44]. Detailed fuel properties for RD5-87 are provided in Table 2.

Table 2. RD5-87 Fuel Specifications

	RD5-87a
Net Heat of Combustion [MJ/kg]	41.639
RON — ASTM D2699	92
MON — ASTM D2700	84.9
Antiknock Index (AKI)	88.5
Sensitivity = Ron – Mon	7.1
Hydrocarbon Type [vol %]	
n-Paraffins	16.868
I-Paraffins	31.76
Aromatics	22.122
Napthenes	11.447
Olefins	6.511
Oxygenates	9.97
Carbon [wt %]	82.26
Hydrogen [wt %]	13.98
Oxygen [wt %]	3.67
A/F Stoichiometric	14.06

Data Acquisition

The pressure transducer signals from the AVL GH15D sensors were digitized and recorded at ¼° CA increments for one hundred consecutive cycles. The cylinder-pressure transducer signal was pegged to the intake pressure near bottom dead center (BDC) where the cylinder pressure reading was virtually constant for several degrees. The CA50 was used to monitor the combustion phasing. CA50 was determined from the cumulative apparent heat-release rate (AHRR), computed from the cylinder-pressure data (after applying a 2.5 kHz low-pass filter [17]. Computations were performed for each individual cycle, disregarding heat transfer and assuming a constant ratio of specific heats [45].[4] The average of 100 consecutive individual-cycle CA50 values were

[4] This specific heat ratio (γ) is determined from a fit to the actual pressure data to account for differences in gas temperature or EGR levels between operating conditions. Comparison of CA50 values computed in this manner with those computed by detailed calculations using real-gas properties that vary over the cycle and a Woschni heat transfer corrections shows good agreement, with differences typically being less than one or two tenths of a degree.

then used to monitor CA50 during engine operation and for the values reported. The reported ringing intensities are computed from the same low-pass-filtered pressure data.

LTGC/HCCI combustion is often limited by high peak-pressure-rise-rates (PPRRs), which can cause acoustic oscillations in the charge gas resulting in audible engine knock. If this phenomenon is not controlled, it can result in unacceptable noise levels and potentially, engine damage. The acceptable knock limit for LTGC engines is often defined in terms of a maximum allowable PRR (dP/dθ, where θ is a variable representing °CA). However, this does not correctly reflect the potential for knock with changes in intake boost or engine speed. In this work, the correlation for ringing intensity (RI) developed by Eng [46] is used as a measure of the propensity for engine knock.

$$RI = \frac{1}{2\gamma} \cdot \frac{\left(0.05 \cdot \left(\frac{dP}{dt}\right)_{max}\right)^2}{P_{max}} \cdot \sqrt{\gamma R T_{max}} \qquad (2)$$

Where $(dP/dt)_{max}$, P_{max}, and T_{max} are the maximum values of PRR in real time (i.e. the PPRR), pressure, and temperature, respectively γ is the ratio of specific heats (c_p/c_v), R is the gas constant, and 0.05 is an empirical correlation constant introduced by Eng which has units of milliseconds. The ringing is a measure of the acoustic energy of the resonating pressure wave that creates the sharp sound commonly known as engine knock. Based on the onset of an audible knocking sound and the appearance of strong ripples on the pressure trace, a ringing criterion of RI = 5 MW/m^2 was selected as the ringing limit for operation without knock. This is the same limit used in our previous works, for example [33, 38] and a more complete discussion of the selection of this value may be found in Ref. [47] This value, 5 MW/m^2, corresponds to about 8 bar/°CA at 1200 rpm, naturally aspirated. However, it should be noted that the allowable PPRR increases with boost due to the increased value of P_{max} in the denominator of Eq. 2. At all boost levels tested, audible engine knock correlated well with the RI rising above 5 MW/m^2, giving confidence in this correlation.

Exhaust emissions data were also acquired, with the sample being drawn from the exhaust plenum using a heated sample line (see Fig.1). CO, CO_2, HC, NOx, O_2, and soot levels were measured using standard exhaust-gas analysis equipment. In addition, a second CO_2 meter monitored the intake gases just prior to induction into the engine. For tests with EGR, this allowed the EGR fraction to be computed from the ratio of the intake and exhaust CO_2 concentrations.

Results and Discussion

CA50 Control Authority using PFS at CR=16:1

Initial investigations of the potential of using PFS for CA50 control were conducted using the CR=16:1 piston (see Fig. 1b). Since gasoline is known to be ϕ-sensitive at boosted intake conditions, the first sweep was performed at P_{in} = 2.0 bar. The CR = 16:1 piston also tends to enhance the ϕ-sensitivity because of the higher compressed-gas pressures, as discussed in the introduction. The global equivalence ratio was set to ϕ_m= 0.40 and the intake temperature (T_{in}) was held constant at 40°C. At these conditions, cooled EGR is necessary to prevent the combustion phasing from becoming overly advanced. The EGR also helps to keep local combustion temperatures from becoming too high as the charge is stratified, mitigating NOx.

Figure 3 demonstrates the ability of double-DI (D-DI) PFS to advance the combustion timing at these operating conditions as the SOI2 is swept from early to late timings. The red curve on this plot is for a 70/30 fuel split, meaning that 70% of the fuel is supplied early in the first DI pulse at 60°CA, and the remaining 30% is injected in the second-DI pulse. The SOI2 timing sweep starts at 200°CA, which gives a relatively well mixed-charge, and at this timing, the amount of EGR was adjusted until CA50 became retarded past 376°CA, at which point the combustion stability began to deteriorate (COV-IMEPg = 3%). Then, the EGR was held constant at this level while the SOI2 was progressively retarded in order to increase the mixture stratification. As can be seen, increasing the stratification with later SOI2s timings can significantly advance CA50 (Fig. 3a), and the COV-IMEPg decreases substantially as CA50 is advanced (Fig. 3b). Initially, the CA50 advancement with increased SOI2 retard was fairly moderate, with CA50 advancing only ~3°CA as SOI2 is retarded from 200°CA to 280°CA. This indicates that stratification is increasing at only a moderate rate for these SOI2s, as might be expected because the cylinder volume is still quite large at these crank angles. However, as the SOI2 is retarded beyond 280°CA, the CA50 advancement for a given change in SOI2 becomes much greater, indicating a significant increase in the rate of stratification. As SOI2 was retarded from 280°CA to 300°CA, CA50 was advanced another 4°CA, at which point the ringing became too high for acceptable engine operation (RI > 5 MW/m^2), as shown in Fig. 3b. Thus, retarding SOI2 from 200°CA to 300°CA gave approximately 7°CA of control authority between the allowable limits of knock (RI = 5 MW/m^2) and stability (COV-IMEPg= 3%). An attempt was made to advance CA50 beyond RI = 5 MW/m^2 to see if CA50 could still be controlled if the engine experienced conditions beyond the optimal range; however, CA50 could only be advanced by 1°CA before runaway knock occurred preventing any further CA50 advancement.

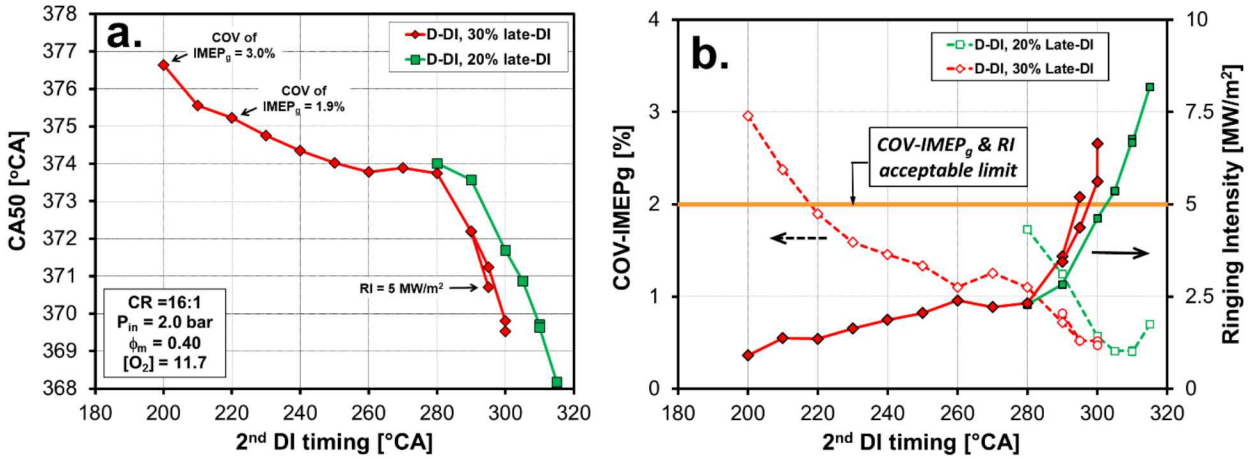

Figure 3. SOI2 timing sweep for a 70/30 and an 80/20 fuel split (a) CA50 Advancement, (b) COV-MEPg and RI

To determine whether changing the injection strategy could increase the total CA50 control range, a SOI2 timing sweep was also performed starting at 280°CA using an 80/20 fuel split (80% at SOI1=60°CA, 20% at SOI2). With a greater fraction of fuel injected earlier, there is less fuel injected in the second pulse, and the SOI2 has to be more retarded to achieve a similar level of stratification and CA50 advancement. The onset of knock (RI ≥ 5 MW/m^2) occurred at around the same CA50 as with the 70/30 split, approximately 371°CA, but with a SOI2 timing of 305°CA. However, with the smaller amount of fuel in the second-DI pulse, combustion remained stable beyond this RI=5 MW/m^2 point and CA50 could be advanced to 368°CA without runaway knock, for a total CA50-control range of about 8.5°CA (see Fig. 3a and 3b).

These results show that D-DI PFS gives good control at P_{in} = 2 bar, with the ability to easily shift CA50 between COV–IMEPg = 3% and RI > 5 MW/m^2. However, it is unknown whether D-DI PFS will continue to be effective as P_{in} was reduced below 2.0 bar since typical gasoline fuels tend to be less ϕ-sensitive at lower intake pressures [32]. To investigate whether D-DI PFS can provide CA50 control at lower P_{in}s, similar SOI2 timing sweeps were performed at P_{in} = 1.6 bar and 1.3 bar, as shown in Fig.4. For these intake pressures, a global equivalence ratio of ϕ=0.36 was used with an 80/20 split because it gave better stability at P_{in} = 1.6 bar as discussed below. For P_{in} = 1.6 bar, the intake temperature was 40°C, the same as for P_{in} = 2.0 bar. Also like P_{in} = 2.0 bar, for a SOI2 = 200°CA, the EGR was adjusted in order to retard CA50 to establish the starting point for the SOI2 timing sweep; however, for P_{in} = 1.6 bar, the CA50 for the starting point was adjusted to give a COV-IMEPg = 2% for greater stability. As the figure shows, retarding SOI2 up to 300°CA advanced CA50 by 4.5°CA, but further SOI2 retard resulted in runaway knock. Attempts to retake the point were unsuccessful, and combustion could not be stabilized with RI ≥ 5 MW/m^2. Increasing the fueling to match the ϕ_m=0.40 value used at P_{in}=2.0 bar increased the tendency for runaway knock, so ϕ_m=0.36 was used for P_{in} = 1.6 and for all other intake pressures, going forward.

Reducing P_{in} to 1.3 bar and below reduces the fuel's autoignition reactivity and T_{in}s > 40°C were required even though no EGR was used. For these lower P_{in}s, starting points of the SOI2 timing sweeps (SOI2 = 200°CA) were established by increasing T_{in} until COV-IMEPg ≈ 2-3%, without using EGR. The T_{in} value for each P_{in} was then held constant throughout the SOI2 timing sweep. For P_{in} = 1.3 bar, T_{in} was set to 72°C. Although ϕ-sensitivity is known to decrease with

lower intake-pressures and higher intake temperatures, Fig. 4 shows that CA50 could still be advanced by 8°CA from the most retarded point, similar to the amount of CA50 control at P_{in}=2.0 bar.

In addition to the P_{in} = 1.3 bar data showing almost the same amount of CA50 control as for P_{in} = 2.0 bar, Fig. 4a shows that the two curves have very similar shapes. The P_{in} = 1.6 bar curve also has a similar shape, up to the SOI2 = 300°CA point, after which combustion became unstable as noted previously (The strong similarly of these three curves is more obvious when they are plotted in an overlaid manner as will be presented in Fig. 6.) This indicates that increasing the fuel stratification is having a similar effect on CA50 up to that point. The reason for this unstable behavior for later SOI2s at P_{in} = 1.6 bar is not understood, but it is thought be related to an anomaly with the GDI fueling at this P_{in} (perhaps a spray collapse) that is giving inconsistent fuel distributions from cycle to cycle. Even for operation with single, early-DI fueling, combustion becomes unstable at P_{in} = 1.6 bar for CR = 16:1. As shown in Dec et al. [38] this unstable behavior limits the maximum fueling to ϕ_m = 0.385 for P_{in} = 1.6 bar when fueling with a single, early-DI, whereas the maximum ϕ_m is 0.43 and 0.42 for P_{in} = 1.0 and 2.0 bar, respectively.

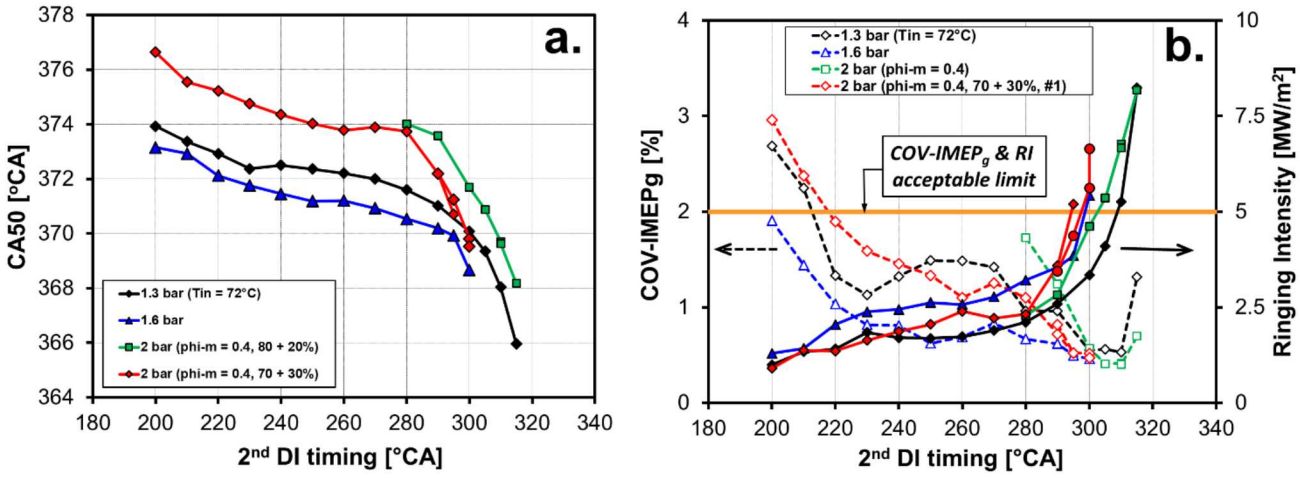

Figure 4. SOI2 timing sweeps, for P_{in} = 2.0 to 1.3 bar. For P_{in} = 2.0 bar ϕ_m = 0.4 and both 70/30 and 80/20 fuel-splits are shown. For P_{in} = 1.6 and 1.3 bar, ϕ=0.36 and an 80/20 fuel-split (a) CA50 Advancement (b) COV-MEPg and RI

Figure 5 extends the investigation of changes in intake pressure from P_{in} = 1.3 bar to naturally aspirated conditions (i.e. P_{in} = 1.0 bar). Because the fuel's autoignition reactivity decreases with reduced P_{in}, progressively more intake heating was required as P_{in} was decreased in order to obtain COV-IMEPg ≈ 2-3% for the start of the sweep with a SOI2 = 200°CA. These T_{in}s are given in the legend of the plots in Fig. 5. As can be seen, the curves from P_{in} = 1.3 – 1.1 bar have similar shapes, and similar CA50 advancement could be achieved as stratification was increased.

However, the P_{in}=1.0 bar curve has a distinctly different shape. For this case, the curve is nearly flat for SOI2s from 200°CA to 240°CA, and CA50 actually becomes slightly more retarded for SOI2s from 240°CA to 270°CA before advancing rapidly at later SOI2s. This fits

with the concept of gasoline not being very ϕ-sensitive at naturally aspirated conditions [18, 32, 35], so the small changes in stratification for SOI2s from 200°CA to 240°CA have little effect. The reason for the small amount of CA50 retard for SOI2s from 240°CA to 270°CA is not well understood, but it could be related to the local charge cooling that occurs with fuel stratification produced by late-DI fueling, which competes with the fuel-chemistry effect of ϕ-sensitivity, as discussed by Dernotte et al. [33]. The regions with the most fuel will be the coldest because they undergo the most vaporization cooling and because γ is lower, resulting in lower compressed temperatures for these higher-fuel regions. The cooling effect would increase for later SOI2s, but if the ϕ-sensitivity is still weak, these cooling effects could dominate, causing CA50 to retard slightly. Then, as SOI2 is further retarded, the increased stratification produces higher local ϕs that increase the fuel-chemistry effect sufficiently for it to dominate over the cooling effect causing CA50 to advance.

With a late-DI retarded past 280°CA, CA50 advances similarly to all of the other curves, but later DI timings are required than for higher P_{in}s to achieve the same CA50 advancement. This suggests that the fuel becomes sufficiently ϕ-sensitive at P_{in} = 1.0 bar if the local equivalence ratios are sufficiently high. Note that lack of significant ϕ-sensitivity at P_{in} = 1.0 bar shown in Ref. [32] is based on measurements that only extend up to a ϕ = 0.47, whereas the most retarded SOI2 point in Fig. 5 results in NOx emissions above the US2010 limit (presented later in Fig. 7), indicating that local equivalence ratios in the stratified mixture extend to at least ~0.7, as explained in Ref. [48]. However, further studies will be required to fully understand the behavior of the CA50 vs. SOI2 curve for P_{in} = 1.0 bar.

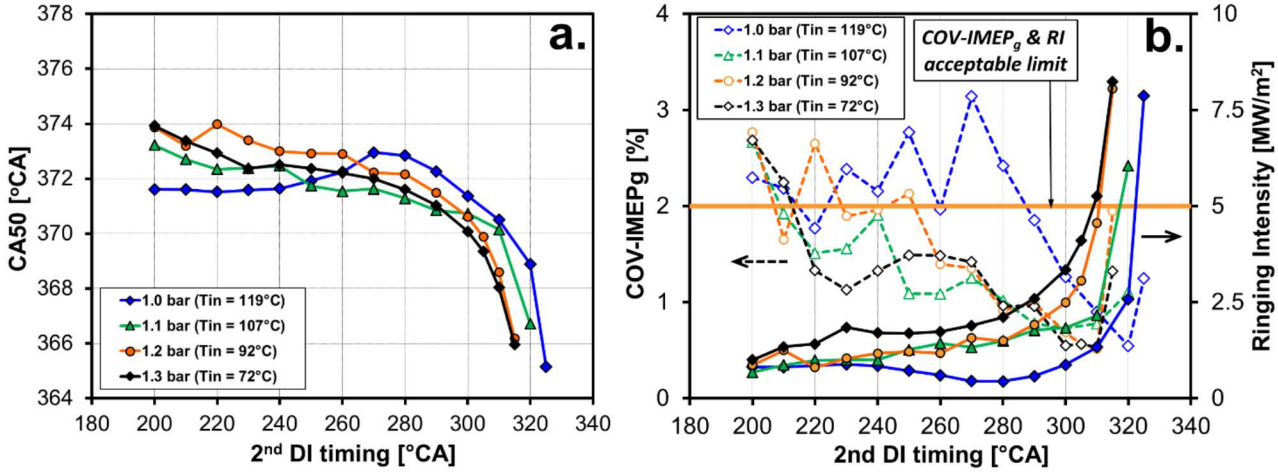

Figure 5. SOI2 timing sweeps for P_{in} = 1.3 bar to 1.0 bar with an 80/20 fuel-split and ϕ_m = 0.36 (a) CA50 Advancement (b) COV-MEPg and RI

Table 2. Summarizes the experimental conditions investigated with the CR=16:1 engine configuration from P_{in}=2.0 bar to 1.0 bar. The range of IMEPg obtained during the SOI2 timing sweeps is also given. Although the fueling rate, airflow, and EGR (for P_{in} = 2.0 and 1.6 bar only) are held constant during each sweep, advancing CA50 increases the expansion ratio thus increasing the amount of work extracted (IMEPg) and the TE. Decreasing boost pressure to P_{in} = 1.3 bar and below required intake heating, which decreases the charge density and the

specific-heat ratio (γ), and increases the heat-transfer losses. These changes act to reduce the IMEP and TE as P_{in} is reduced.

Table 2. Summary of Experimental conditions for CR=16:1

Intake Pressure	Intake Temperature	Oxygen Concentration	Equivalence Ratio	Range of IMEPg as SOI2 varies	Indicated TEs
2.0 bar	40°C	11.66%	ϕ_m = 0.40	11.44 to 12.13 bar	45.5 to 48.0%
1.6 bar	40°C	17.26%	ϕ_m = 0.36	8.51 to 8.73 bar	46.5 to 47.7%
1.3 bar	73°C	20.95%	ϕ_m = 0.36	6.10 to 6.32 bar	44.9 to 46.2%
1.2 bar	92°C	20.95%	ϕ_m = 0.36	5.34 to 5.60 bar	43.9 to 45.8%
1.1 bar	107°C	20.95%	ϕ_m = 0.36	4.74 to 4.88 bar	43.4 to 44.7%
1.0 bar	119°C	20.95%	ϕ_m = 0.36	4.09 to 4.27 bar	42.5 to 44.3%

Since the experimental conditions vary significantly for the range of intake pressures tested, and because the CA50 for the starting point of the sweeps varies (the sweeps start with a CA50 that gives COV-IMEPg~2-3%, which inherently has some variability), the curves in Figs. 4a and 5a were offset to align the SOI2 = 280°CA points, and replotted in Fig. 6. To account for the offset, the y-axis of Fig. 6 shows the difference between the actual CA50 and the CA50 for SOI2 = 280°CA. This collapses the series of curves onto a single point for the SOI2 at 280°CA, and allows for an easier comparison of shape of the curves over the DI-timing sweep for all the intake pressures investigated. The two fueling strategies at P_{in}=2.0 bar have been combined into a single curve with the 70/30 fuel-split data being plotted from 200°CA to 280°CA, and the 80/20 data points plotted from 280°CA-315°CA. Most of the curves have a remarkably similar profile, showing a shallow advancement of CA50 for early to intermediate SOI2s (200 to ~280°CA), followed by a more pronounced CA50 advancement as the SOI2 is retarded past ~280°CA. For P_{in}s from 2.0 to 1.2 bar, the shape of the curves is nearly identical. However, for P_{in} = 1.1 bar, for SOI2s > 290°CA, SOI2 must be retarded further to achieve the same CA50 advancement as the higher P_{in}s, presumably because the fuel is becoming less ϕ-sensitive at this lower P_{in}. At P_{in}=1.0 bar curve shape becomes distinctly different as discussed above with respect to Fig. 5. However, as noted above, when the SOI2 is retarded past 280°CA, CA50 can be advanced by almost 8°CA without runaway knock, almost the same as the entire CA50 advancement range for the other intake pressures.

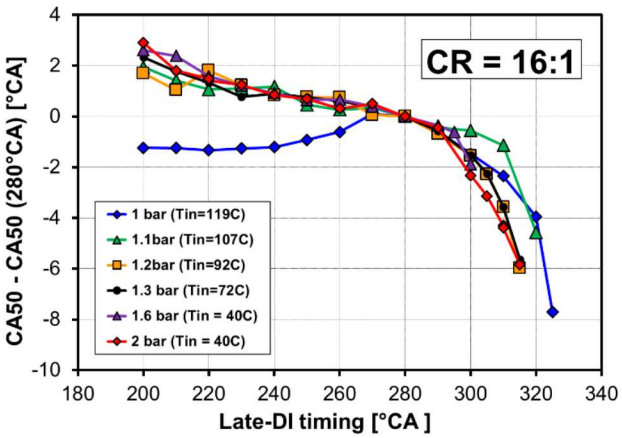

Figure 6. SOI2 timing sweeps for P_{in} = 2 bar to 1.0 bar showing relative CA50 advance (CA50 minus the CA50 obtained with SOI2 = 280°CA).

Figure 7 shows the NOx and soot emissions for the SOI2 timing sweeps at CR=16:1 presented above in Figs 4 – 6. For the majority of the SOI2s, NOx and soot emissions are almost zero; the NOx axis limit was plotted with an offset to separate the NOx and soot curves. As SOI2 is retarded beyond 300°CA, NOx begins to increase and extends above the 2010 US HD limit (0.27 g/kw-hr) at the most stratified conditions (i.e. late SOI2s) for the conditions that required intake heating. For the boosted conditions that had a lower T_{in} = 40°C and required EGR (P_{in}=2.0 bar and P_{in}=1.6 bar), NOx emissions remained well below the 2010 mandated values. For all conditions at CR=16:1, soot remained well below the legal limit (0.14 g/kw-hr).

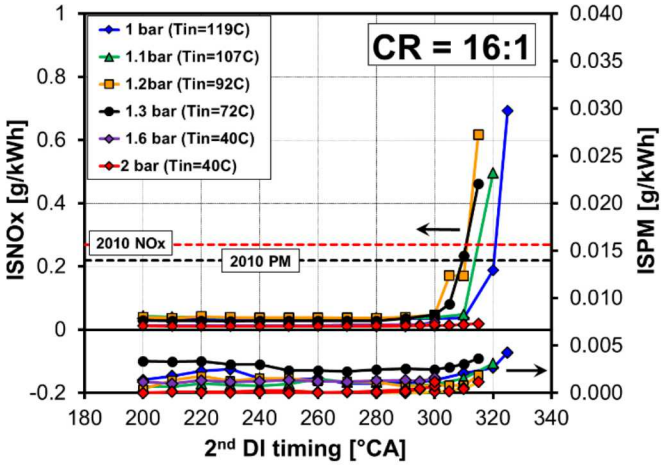

Figure 7. NOx and soot emissions for the CR=16:1 SOI2 timing sweep from P_{in} = 2.0 bar to 1.0 bar.

Figure 8. reports the total amount of CA50 control authority from the most retarded CA50 (COV-IMEPg~2-3%), to the most advanced CA50 limited by runaway knock (RI > 5 MW/m2) or high NOx emissions. The baseline is COV-IMEPg = 2%, which is considered an acceptable value for

engine operation. Although COV-IMEPg > 2% is not an ideal operating point due to the possibility of partial burn or misfire cycles, the engine is still stable ad capable of being shifted back to a more ideal phasing, so these CA50s are included in the total range. Similarly, the most advanced CA50 that can be obtained with steady combustion conditions (i.e. no runaway knock) defines the upper CA50 control limit. Since the onset of knocking occurs at RI > 5 MW/m^2, a more advanced CA50 would lead to engine knock, and operation should avoid operating in the region for extended periods to avoid engine damage and to keep engine noise levels low. However, if the engine is already knocking, it is important for a given control technique to be able to quickly shift the CA50 back into the desired operating range, i.e. the range where COV-IMEPg ≤ 2% and RI ≤ $5MW/m^2$.

Emissions are also a constraint on the allowable CA50 advance. As shown in Fig. 7, if the mixture becomes too stratified, NOx emissions can become high, reaching levels above the US 2010 HD legal limit = 0.27 g/kw-hr. This is primarily from the thermal NOx formation mechanism as the combustion temperatures increase due to the local equivalence ratios become higher for late SOI2s. In Ref. [48], a rapid rise in NOx emissions occurred when the local equivalence increased above ϕ_m = 0.7, determined by fuel distribution measurements in an optical engine. The exact equivalence ratio corresponding to the "NOx-knee" will depend on the engine conditions, but this gives a first order estimate of the highest local ϕ_m in the cylinder when the NOx increases substantially. Soot formation occurs with a much higher local equivalence ratio of ϕ_m above ~2, which is the reason soot emissions remain low for this work since the stratification levels were not increased much past the NOx limit corresponding to $\phi_m \approx 0.7$.

With the CR = 16:1 piston, the maximum CA50 advance from P_{in} = 1.0 to 1.3 bar were limited by high NOx. For the P_{in} = 1.6 bar and 2.0 bar, NOx emissions remained below the legal limit because of the lower T_{in} and the presence of EGR, but the maximum CA50 advance was limited by runaway knock. Only the P_{in}=1.0 bar and 1.3 bar continued to be stable for the most advanced CA50, so further control is possible for these conditions, but with a NOx penalty. Notably, runaway knock occurred with less CA50 advance for P_{in}=1.6 bar, so CA50 could only be advanced by 4.5°CA, much less than the 6.5°-8.5°CA range shown for the other intake pressures tested. As discussed above with respect to Fig. 4, this instability is thought to be caused by the mixture formation at these conditions.

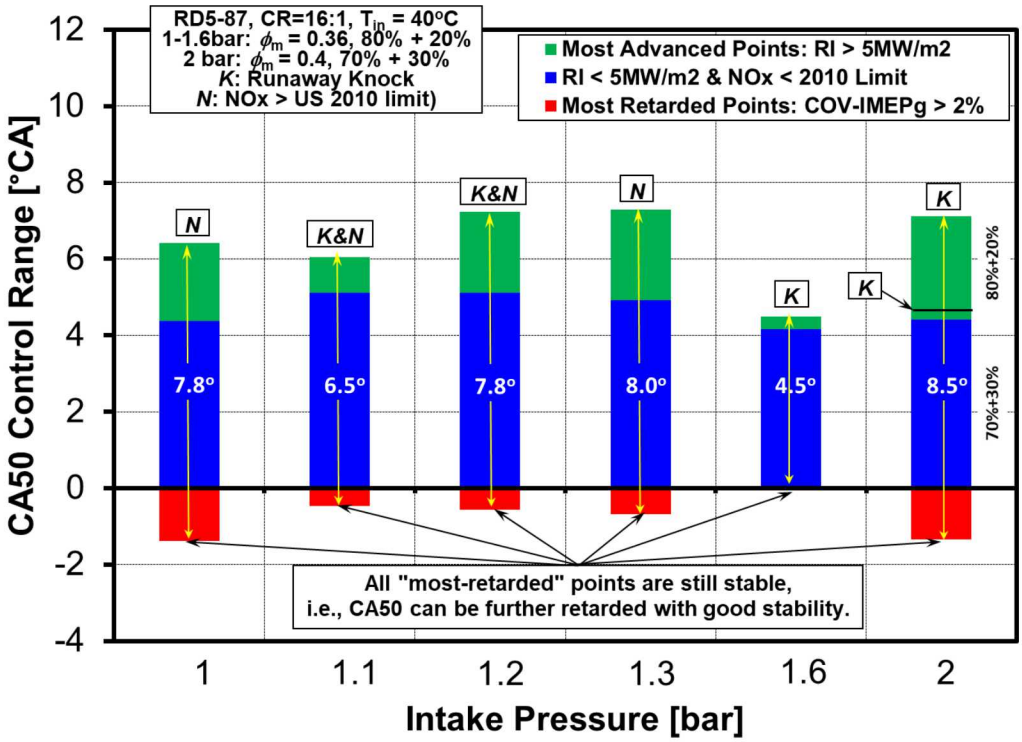

Figure 8. Maximum amount of CA50 control possible at 16:1 CR, and factors limiting this range.

CA50 Control Authority using PFS at CR=14:1

This section presents the amount of CA50 control obtained using PFS with the CR =14:1 piston shown in Fig. 1b. With a lower compression ratio, there is less compression from the piston, requiring less EGR at the higher boost pressures to prevent CA50 from becoming too advanced. Conversely, less compression from the piston also means that more intake heating is required from P_{in}=1.0 bar to 1.6 bar to compensate for the lower compressed-gas pressures and temperatures. Table 3 gives a summary of the experimental conditions used for the SOI2 timing sweeps with CR=14:1.

Table 3. Summary of CR = 14:1 Experimental Conditions

Intake Pressure	Intake Temperature	Oxygen Concentration	Equivalence Ratio	Range of IMEPg as SOI2 varies	Indicated TEs
2.4 bar	40°C	13.11%	ϕ_m = 0.36	11.77 to 12.52 bar	44.6 to 47.3%
2.0 bar	40°C	16.54%	ϕ_m = 0.36	10.30 to 10.74 bar	45.3 to 47.2%
1.6 bar	61°C	20.95%	ϕ_m = 0.36	7.55 to 7.77 bar	45.1 to 46.5%
1.3 bar	127°C	20.95%	ϕ_m = 0.36	5.18 to 5.40 bar	43.0 to 44.9%
1.2 bar	135°C	20.95%	ϕ_m = 0.36	4.73 to 4.89 bar	42.3 to 44.2%
1.1 bar	147°C	20.95%	ϕ_m = 0.36	4.14 to 4.30 bar	41.9 to 43.7%
1.0 bar	159°C	20.95%	ϕ_m = 0.36	3.77 to 3.88 bar	41.7 to 43.3%

Figure 9. shows the CA50 relative to CA50 with SOI2 = 280°CA, for intake pressures from P_{in}= 1.0-2.4 bar. With SOI2 from 200°-280° CA, the CA50s corresponding to P_{in}=1.0 bar became slightly retarded, similar to what was seen with the CR=16:1 results. During this SOI2 timing window, P_{in}=1.1 and 1.2 bar also showed very little response in CA50 from varying the SOI2. For P_{in} > 1.3 bar, CA50 advances with a SOI2 from 200°-280° CA. P_{in}=1.3 bar and 1.6 bar seem to be grouped together, as well as P_{in}=2.0 bar and 2.4 bar. This seems to suggest that either that the changes in phi-sensitivity are offset by changes to the amount of stratification, or that the phi-sensitivity and stratification levels are not changing much at these conditions.

For a SOI2 more retarded than 280°CA, CA50 advances for all intake pressures to varying degrees. Lower intake pressures required a more retarded SOI2 to advance the combustion timing, with less total CA50 advancement before forming NOx, as seen in Fig.10. NOx emissions began to become significant for SOI2s more retarded than 310°CA, but the RI remained less than 5 MW/m^2 without runaway knock. The RI for all intake pressures are shown in Fig. 11. To test the combustion stability at Pin = 1.6 bar, which quickly ran away to knocking at CR=16:1, the SOI2 was retarded past 320°CA, further advancing CA50 and increasing the ringing. Although the NOx values were above the legal limit with a high RI (7.5 MW/m2), CA50 remained steady and controllable. Thus, the total controllable range of CA50 for Pin=1.6 bar with a CR=14:1 was measured to be 12°CA. This is much greater than the 4.5°CA of CA50 control with CR=16:1. Although this conditions was stable, with Pin=2.0 and 2.4 bar the amount of CA50 advance was again limited by runaway knock. It is interesting to note that these two conditions required EGR, while the more stable conditions did not. The reason why some conditions experience runaway knock, while others are quite stable even with a high RI is another aspect that is not well understood and warrants further study. NOx emissions remained low for P_{in}=1.6 and 2.0 bar, and soot emissions remained well below the legal limit for all intake pressures, with a slight trend upward with the most retarded SOI2s.

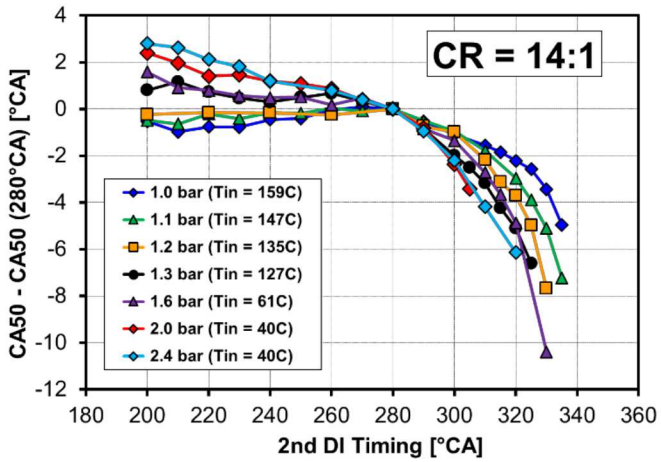

Figure 9. CA50 relative to CA50 with SOI2= 280°CA for the SOI2 timing sweeps from P_{in} = 2.4 bar to 1.0 bar. CR=14:1, P_{in}=1.0-2.4 bar, ϕ=0.36, 80/20 fuel split.

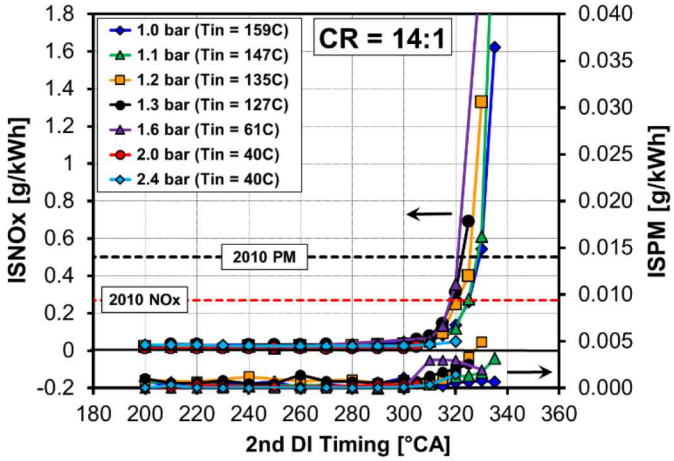

Figure 10. NOx and soot emissions for CR=14:1 for the SOI2 timing sweeps from P_{in} = 2.4 bar to 1.0 bar. US 2010 HD NOx limit = 0.27 g/kw-hr. US 2010 HD PM limit = 0.14 g/kw-hr.

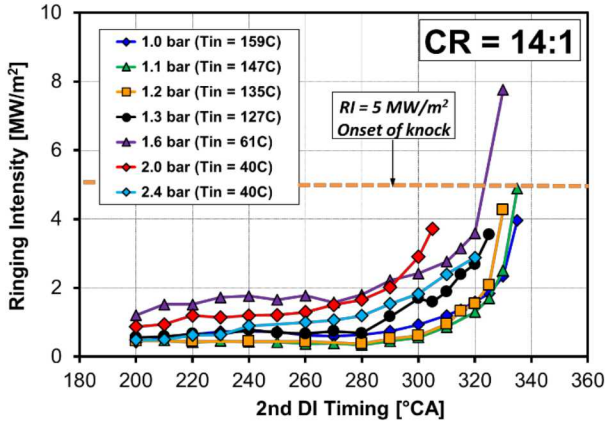

Figure 11. Ringing intensity for CR=14:1 SOI2 timing sweep from P_{in} = 2.4 bar to 1.0 bar.

Figure 12 Summarizes the amount of CA50 control obtained with the CR=14:1 piston. The CA50 control range between the desired operating window of COV-IMEPg = 2% and RI = 5 MW/m^2 is narrower compared to CR=16:1 for some conditions with 3.5°-8.9°CA of CA50 control authority. P_{in}=2.0 and 2.4 bar displayed a greater range of CA50 in this desired operating window compared to CR=16:1, but the amount of CA50 advancement was limited by runaway knock preventing CA50 from advancing any further. For $P_{in} \leq$ 1.6 bar, approximately 6°-8°CA of CA50 control could be obtained with RI < 5 MW/m^2 and steady operation, with greater CA50 control with high RI and NOx, as demonstrated by the larger CA50 range of 12°CA at P_{in}=1.6 bar.

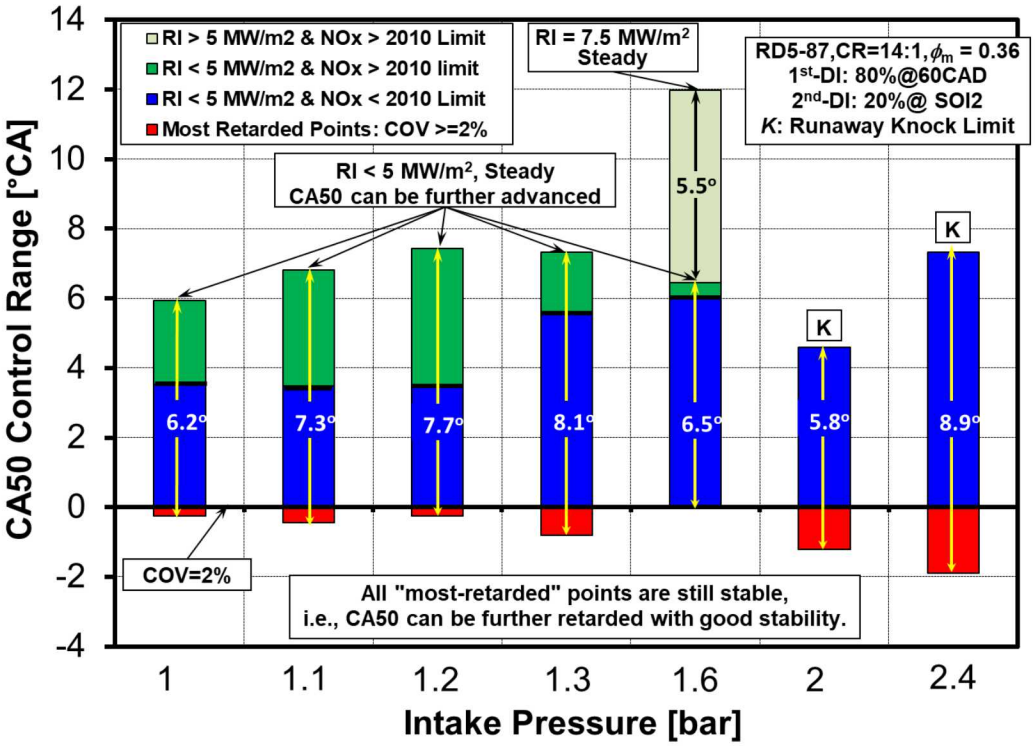

Figure 12. Maximum amount of CA50 control possible with CR = 14:1.

Summary and Conclusions

This paper explores the potential of D-DI PFS to provide fast control of CA50 in an LTGC engine for two different compression ratios (CR=16:1 and 14:1) using a research grade E10 gasoline (RON 92, MON 85) representative of a market gasoline found in the United States. Compression ratios in this range provide high efficiencies (measured in this paper to be 42.5%-48%, indicated). For both compression ratios, a second injection (SOI2) timing sweep was performed at several intake pressures from highly boosted to naturally aspirated conditions. Varying the level of fuel stratification for each condition by sweeping the injection timing showed that PFS could effectively control the CA50, even at naturally aspirated conditions where gasoline has been considered to not be very sensitive to changes in the local ϕ (i.e. not very ϕ-sensitive). Furthermore, at a given CR, some intake pressures were found to be more stable than others. PFS applied at certain intake pressures experienced runaway knock preventing CA50 from advancing further, while at other intake pressures CA50 could be advanced with good stability to conditions resulting in a high RI (i.e. strong knock) and high NOx.

- At CR=16:1, approximately 6.5° - 8.5°CA of CA50 control authority was possible with good stability from the most retarded to the most advanced CA50 for all P_{in}s from 2.0 to 1.0 bar, except 1.6 bar where control was limited to 4.5°CA. With this CR, NOx increased above the US 2010 HD legal limit only for $P_{in} \leq 1.3$ bar, corresponding to conditions that required intake heating. For P_{in} =1.6 and 2.0 bar NO_x emissions remained well below the mandated levels.
- At CR=16:1, at P_{in} = 2.0 bar, changing from a 70/30 to an 80/20 fuel split improved the combustion stability for later SOI2s.This suggests that significant improvement in CA50 control is likely by optimizing the mixture formation strategy.
- At CR=16:1, the shapes of the CA50 advancement curves with SOI2 timing were very similar for all intake pressures, except P_{in} = 1.0 bar did not show CA50 advancement until SOI2 was retarded beyond 280°CA. It appears that at naturally aspirated conditions, gasoline might become ϕ-sensitve with enough stratificaiton, but future studies are needed to understand and accurately characterize this behavior.
- At CR=14:1, approximately 5.8° - 8.9°CA of CA50 control authority was possible with good stability from the most retarded to the most advanced CA50. The most advanced CA50s were limited either by high NOx or runaway knock depending on P_{in}, even though RI remained < 5 MW/m^2.
- At CR=14:1, the shapes of the CA50 vs. SOI2 curves change progressively as P_{in} is reduced from 2.4 to 1.0 bar, in contrast to CR = 16:1 where all the curves have very similar shapes except for P_{in} = 1.0 bar. As P_{in} is reduced, the CA50 advancement for SOI2s from 200 – 280°CA is progressively reduced, with no CA50 advancement at all occuring for $P_{in} \leq 1.2$ bar, and for SOI2 > 280°CA, progressively more SOI2 retard is required to achieve the same CA50 advancement for $P_{in} \leq 1.2$ bar. These changes are consistent with the ϕ-sensitivity decreasing more rapidly with reduced P_{in} at CR-14:1.
- With CR=14:1, as CA50 was advanced by increased stratification, the NOx limit was reached while the RI was still < 5 MW/m^2 for P_{in}=1.0-1.6 bar, without experincing runaway knock. However, the maximum CA50 advance was limited by runaway knock at P_{in}=2.0 and 2.4 bar.
- At P_{in}=1.6 bar, the total CA50 control range was measured to be 12°CA, with steady operation but with high NOx and RI > 5MW/m^2. PFS applied at the same intake pressure for the CR=16:1 conditions were much less stable, resulting in only 4.5°CA of CA50 control. Understanding why some conditions lead to runaway knock while others do not requires further investigation.
- Soot emissions remained well below the US 2010 legal limit (0.014 g/kw-hr) for all conditons at both CR =14:1 and CR=16:1.

This work has shown that using a practicable engine configuration and operating parameters with a regular E10 gasoline, PFS can be applied to provide rapid CA50 control in an LTGC engine for intake pressures from high-boost to naturally aspirated. There is significant scope for improvement in combustion-timing control and managing emissions by optimizing the injection strategies used.

Contact Information

Corresponding author:

John E. Dec
Sandia National Laboratories
MS 9053, PO Box 969
Livermore, CA 94551-0968, USA

Acknowledgements

The authors would like to thank Tim Gilbertson, Keith Penney, Gary Hubbard, and Alberto Garcia for their dedicated support of the LTGC Engine Laboratory.

This work was performed at the Combustion Research Facility, Sandia National Laboratories, Livermore, CA, Support was provided by the U.S. Department of Energy, Office of Vehicle Technologies. Sandia National Laboratories is a multi-mission laboratory managed and operated by National Technology and Engineering Solutions of Sandia, LLC., a wholly owned subsidiary of Honeywell International, Inc., for the U.S. Department of Energy's National Nuclear Security Administration under contract DE-NA0003525.

Definitions/Abbreviations

aTDC	after top dead center
AHRR	apparent heat release rate
AKI	Anti-Knock Index = (RON + MON)/2
BDC	bottom dead center
bTDC	before top dead center
CA	crank angle
°CA	crank angle degrees
CA50	crank angle of 50% burn point
CI	compression ignition
CR	compression ratio
CO	carbon monoxide
CO_2	carbon dioxide
COV	coefficient of variation
DI	direct injection
DHA	detailed hydrocarbon analysis

E10	10% Ethanol
EGR	exhaust gas recirculation
GDI	gasoline direct injector
HC	hydrocarbon
HCCI	homogeneous charge compression ignition – a well premixed form of LTGC
HRR	heat release rate
$IMEP_g$	gross indicated mean effective pressure
ISNOx	indicated specific NOx
LTGC	low temperature gasoline combustion
MON	Motor Octane Number
O_2	oxygen
P_{in}	intake pressure
PLIF	Planar Laser Induced Fluorescence
PM	particulate matter
PRR	pressure rise rate
PPRR	peak pressure rise rate
RD5-87	research-quality, regular-grade E10 gasoline. Specifications in Table 2.
RI	ringing intensity, see Eq. 2
RON	research octane number
RPM	revolutions per minute
SA	spark assist
SOI1	Start of injection of first fuel pulse
SOI2	Start of injection of second fuel pulse
T_{in}	intake temperature
TDC	top dead center
NO_x	oxides of nitrogen

References

1. Dec, J. E., Y. Yang, and N. Dronniou, "*Improving Efficiency and Using E10 for Higher Loads in Boosted HCCI Engines.*" SAE International Journal of Engines, 2012. **5**(3): p. 1009-1032 DOI:10.4271/2012-01-1107
2. Manente, V., B. Johansson, P. Tunestal, and W. Cannella, "*Effects of Different Type of Gasoline Fuels on Heavy Duty Partially Premixed Combustion.*" SAE International Journal of Engines, 2009. **2**(2): p. 71-88 DOI:https://doi.org/10.4271/2009-01-2668
3. Kawamoto, K., O. Aoki, H. Ogawa, and S. Kimura, "*Improvement of output performance of a DI diesel engine with the MK combustion concept*". 2000, Society of Automotive Engineers of Japan
4. Hasegawa, R. and H. Yanagihara, "*HCCI Combustion in DI Diesel Engine*". 2003, SAE International DOI:https://doi.org/10.4271/2003-01-0745.
5. Yang, Y., J. E. Dec, N. Dronniou, and B. Simmons, "*Characteristics of Isopentanol as a Fuel for HCCI Engines.*" SAE International Journal of Fuels and Lubricants, 2010. **3**(2): p. 725-741 DOI:https://doi.org/10.4271/2010-01-2164
6. Dec, J. E., *Advanced Compression-Ignition Combustion for High Efficiency and Ultra-Low NOX and Soot*, in *Encyclopedia of Automotive Engineering*. 2014, John Wiley & Sons, Ltd DOI:10.1002/9781118354179.auto121.
7. Dec, J. E., "*Advanced compression-ignition engines—understanding the in-cylinder processes.*" Proceedings of the Combustion Institute, 2009. **32**(2): p. 2727-2742 DOI:https://doi.org/10.1016/j.proci.2008.08.008
8. Dronniou, N. and J. E. Dec, "*Investigating the Development of Thermal Stratification from the Near-Wall Regions to the Bulk-Gas in an HCCI Engine with Planar Imaging Thermometry.*" SAE International Journal of Engines, 2012. **5**(3): p. 1046-1074 DOI:10.4271/2012-01-1111
9. Sjöberg, M., J. E. Dec, A. Babajimopoulos, and D. N. Assanis, "*Comparing Enhanced Natural Thermal Stratification Against Retarded Combustion Phasing for Smoothing of HCCI Heat-Release Rates*". 2004, SAE International DOI:10.4271/2004-01-2994.
10. Dec, J. E., W. Hwang, and M. Sjöberg, "*An Investigation of Thermal Stratification in HCCI Engines Using Chemiluminescence Imaging*". 2006, SAE International DOI:https://doi.org/10.4271/2006-01-1518.
11. Onishi, S., S. H. Jo, K. Shoda, P. D. Jo, and S. Kato, "*Active Thermo-Atmosphere Combustion (ATAC) - A New Combustion Process for Internal Combustion Engines*". 1979, SAE International DOI:https://doi.org/10.4271/790501.
12. Najt, P. M. and D. E. Foster, "*Compression-Ignited Homogeneous Charge Combustion*". 1983, SAE International DOI:https://doi.org/10.4271/830264.
13. Yang, Y., J. E. Dec, N. Dronniou, M. Sjöberg, and W. Cannella, "*Partial Fuel Stratification to Control HCCI Heat Release Rates: Fuel Composition and Other Factors Affecting Pre-Ignition Reactions of Two-Stage Ignition Fuels.*" SAE International Journal of Engines, 2011. **4**(1): p. 1903-1920 DOI:https://doi.org/10.4271/2011-01-1359
14. Koopmans, L. and I. Denbratt, "*A Four Stroke Camless Engine, Operated in Homogeneous Charge Compression Ignition Mode with Commercial Gasoline*". 2001, SAE International DOI:https://doi.org/10.4271/2001-01-3610.
15. Law, D., D. Kemp, J. Allen, G. Kirkpatrick, and T. Copland, "*Controlled Combustion in an IC-Engine with a Fully Variable Valve Train*". 2001, SAE International DOI:https://doi.org/10.4271/2001-01-0251.
16. Sjöberg, M., J. E. Dec, and W. Hwang, "*Thermodynamic and Chemical Effects of EGR and Its Constituents on HCCI Autoignition*". 2007, SAE International DOI:https://doi.org/10.4271/2007-01-0207.

17. Dec, J. E. and M. Sjöberg, "*A Parametric Study of HCCI Combustion - the Sources of Emissions at Low Loads and the Effects of GDI Fuel Injection*". 2003, SAE International DOI:10.4271/2003-01-0752.
18. Dec, J. E. and M. Sjöberg, "*Isolating the Effects of Fuel Chemistry on Combustion Phasing in an HCCI Engine and the Potential of Fuel Stratification for Ignition Control*". 2004, SAE International DOI:https://doi.org/10.4271/2004-01-0557.
19. Sjöberg, M. and J. E. Dec, "*Smoothing HCCI Heat-Release Rates Using Partial Fuel Stratification with Two-Stage Ignition Fuels*". 2006, SAE International DOI:https://doi.org/10.4271/2006-01-0629.
20. Kalghatgi, G. T., P. Risberg, and H.-E. Ångström, "*Advantages of Fuels with High Resistance to Auto-ignition in Late-injection, Low-temperature, Compression Ignition Combustion*". 2006, SAE International DOI:https://doi.org/10.4271/2006-01-3385.
21. Kalghatgi, G. T., P. Risberg, and H.-E. Ångström, "*Partially Pre-Mixed Auto-Ignition of Gasoline to Attain Low Smoke and Low NOx at High Load in a Compression Ignition Engine and Comparison with a Diesel Fuel*". 2007, SAE International DOI:https://doi.org/10.4271/2007-01-0006.
22. Hildingsson, L., G. Kalghatgi, N. Tait, B. Johansson, and A. Harrison, "*Fuel Octane Effects in the Partially Premixed Combustion Regime in Compression Ignition Engines*". 2009, SAE International DOI:https://doi.org/10.4271/2009-01-2648.
23. Kalghatgi, G., L. Hildingsson, and B. Johansson, "*Low NOx and Low Smoke Operation of a Diesel Engine Using Gasolinelike Fuels.*" Journal of Engineering for Gas Turbines and Power, 2010. **132**(9): p. 092803-092803-9 DOI:10.1115/1.4000602
24. Manente, V., C.-G. Zander, B. Johansson, P. Tunestal, and W. Cannella, "*An Advanced Internal Combustion Engine Concept for Low Emissions and High Efficiency from Idle to Max Load Using Gasoline Partially Premixed Combustion*". 2010, SAE International DOI:https://doi.org/10.4271/2010-01-2198.
25. Shen, M., S. Lonn, and B. Johansson, "*Transition from HCCI to PPC Combustion by Means of Start of Injection*". 2015, SAE International DOI:https://doi.org/10.4271/2015-01-1790.
26. Vedharaj, S., R. Vallinayagam, Y. An, M. Izadi Najafabadi, B. Somers, J. Chang, and B. Johansson, "*Combustion Homogeneity and Emission Analysis during the Transition from CI to HCCI for FACE I Gasoline*". 2017, SAE International DOI:https://doi.org/10.4271/2017-01-2263.
27. An, Y., M. J. Mubarak Ali, R. Vallinayagam, A. AlRamadan, J. Sim, J. Chang, H. Im, and B. Johansson, "*Compression Ignition of Low Octane Gasoline under Partially Premixed Combustion Mode*". 2018, SAE International DOI:https://doi.org/10.4271/2018-01-1797.
28. Sellnau, M., W. Moore, J. Sinnamon, K. Hoyer, M. Foster, and H. Husted, "*GDCI Multi-Cylinder Engine for High Fuel Efficiency and Low Emissions.*" SAE International Journal of Engines, 2015. **8**(2): p. 775-790 DOI:https://doi.org/10.4271/2015-01-0834
29. Sellnau, M., K. Hoyer, W. Moore, M. Foster, J. Sinnamon, and W. Klemm, "*Advancement of GDCI Engine Technology for US 2025 CAFE and Tier 3 Emissions*". 2018, SAE International DOI:https://doi.org/10.4271/2018-01-0901.
30. Yang, Y., J. E. Dec, N. Dronniou, and M. Sjöberg, "*Tailoring HCCI heat-release rates with partial fuel stratification: Comparison of two-stage and single-stage-ignition fuels.*" Proceedings of the Combustion Institute, 2011. **33**(2): p. 3047-3055 DOI:https://doi.org/10.1016/j.proci.2010.06.114
31. Sjoberg, M. and J. E. Dec, "*Smoothing HCCI Heat Release with Vaporization-Cooling-Induced Thermal Stratification using Ethanol.*" SAE International Journal of Fuels and Lubricants, 2011. **5**(1): p. 7-27 DOI:https://doi.org/10.4271/2011-01-1760
32. Dec, J. E., Y. Yang, and N. Dronniou, "*Boosted HCCI - Controlling Pressure-Rise Rates for Performance Improvements using Partial Fuel Stratification with Conventional Gasoline.*" SAE

International Journal of Engines, 2011. **4**(1): p. 1169-1189 DOI:https://doi.org/10.4271/2011-01-0897

33. Dernotte, J., J. Dec, and C. Ji, "*Efficiency Improvement of Boosted Low-Temperature Gasoline Combustion Engines (LTGC) Using a Double Direct-Injection Strategy*". 2017, SAE International DOI:10.4271/2017-01-0728.
34. Sjöberg, M. and J. E. Dec, "*An investigation into lowest acceptable combustion temperatures for hydrocarbon fuels in HCCI engines.*" Proceedings of the Combustion Institute, 2005. **30**(2): p. 2719-2726 DOI:https://doi.org/10.1016/j.proci.2004.08.132
35. Yang, Y., J. E. Dec, N. Dronniou, and W. Cannella, "*Boosted HCCI Combustion Using Low-Octane Gasoline with Fully Premixed and Partially Stratified Charges.*" SAE International Journal of Engines, 2012. **5**(3): p. 1075-1088 DOI:10.4271/2012-01-1120
36. Hwang, W., J. Dec, and M. Sjöberg, "*Spectroscopic and chemical-kinetic analysis of the phases of HCCI autoignition and combustion for single- and two-stage ignition fuels.*" Combustion and Flame, 2008. **154**(3): p. 387-409 DOI:https://doi.org/10.1016/j.combustflame.2008.03.019
37. Gentz, G., J. Dernotte, C. Ji, and J. Dec, "*Spark Assist for CA50 Control and Improved Robustness in a Premixed LTGC Engine – Effects of Equivalence Ratio and Intake Boost*". 2018, SAE International DOI:https://doi.org/10.4271/2018-01-1252.
38. Dec, J. E., J. Dernotte, and C. Ji, "*Increasing the Load Range, Load-to-Boost Ratio, and Efficiency of Low-Temperature Gasoline Combustion (LTGC) Engines.*" SAE International Journal of Engines, 2017. **10**(3): p. 1256-1274 DOI:10.4271/2017-01-0731
39. Manofsky, L., J. Vavra, D. N. Assanis, and A. Babajimopoulos, "*Bridging the Gap between HCCI and SI: Spark-Assisted Compression Ignition*". 2011, SAE International DOI:10.4271/2011-01-1179.
40. Koopmans, L., H. Ström, S. Lundgren, O. Backlund, and I. Denbratt, "*Demonstrating a SI-HCCI-SI Mode Change on a Volvo 5-Cylinder Electronic Valve Control Engine*". 2003, SAE International DOI:https://doi.org/10.4271/2003-01-0753.
41. Dec, J. E. and Y. Yang, "*Boosted HCCI for High Power without Engine Knock and with Ultra-Low NOx Emissions - using Conventional Gasoline.*" SAE International Journal of Engines, 2010. **3**(1): p. 750-767 DOI:https://doi.org/10.4271/2010-01-1086
42. Dec, J. E., Y. Yang, J. Dernotte, and C. Ji, "*Effects of Gasoline Reactivity and Ethanol Content on Boosted, Premixed and Partially Stratified Low-Temperature Gasoline Combustion (LTGC).*" SAE International Journal of Engines, 2015. **8**(3): p. 935-955 DOI:10.4271/2015-01-0813
43. Dec, J. E. and Y. Yang, "*Boosted HCCI for High Power without Engine Knock and with Ultra-Low NOx Emissions - using Conventional Gasoline.*" SAE Int. J. Engines, 2010. **3**(1): p. 750-767 DOI:10.4271/2010-01-1086
44. Vuilleumier, D., N. Kim, M. Sjöberg, N. Yokoo, T. Tomoda, and K. Nakata, "*Effects of EGR Constituents and Fuel Composition on DISI Engine Knock: An Experimental and Modeling Study*". 2018, SAE International https://doi.org/10.4271/2018-01-1677.
45. Heywood, J. B., "*Internal combustion engine fundamentals*". 1988: New York : McGraw-Hill, [1988] ©1988
46. Eng, J. A., "*Characterization of Pressure Waves in HCCI Combustion*". 2002, SAE International 10.4271/2002-01-2859.
47. Dernotte, J., J. E. Dec, and C. Ji, "*Energy Distribution Analysis in Boosted HCCI-like / LTGC Engines - Understanding the Trade-Offs to Maximize the Thermal Efficiency.*" SAE International Journal of Engines, 2015. **8**(3): p. 956-980 DOI:10.4271/2015-01-0824
48. Hwang, W., J. E. Dec, and M. Sjöberg, "*Fuel Stratification for Low-Load HCCI Combustion: Performance & Fuel-PLIF Measurements.*" SAE Transactions, 2007. **116(3)**: p. 1437-1460 DOI:https://doi.org/10.4271/2007-01-4130